Water Qual Expo Health (2015) 7:5–14
DOI 10.1007/s12403-013-0101-7

Assessment and Transport of Sediment-Bound Estuarine Contaminants

P.A. Work · K.A. Haas · D.A. Warren · Ş. Elci

Received: 30 May 2013 / Accepted: 17 October 2013 / Published online: 7 November 2013

Abstract Estuaries and coastal bays frequently receive anthropogenically sourced contaminants. Many of these contaminants (e.g. most metals) have low solubility and tend to sorb to sediment particles, so that sediment transport driven by fluid mechanics becomes an important part of the contaminant transport problem. The chosen strategy for mitigation of the contaminant(s) will depend on the potential for migration away from the affected region, or the build-up of concentrations within the receiving area if loading rate exceeds decay or transport rates, and the potential impact on environmental and human health both within and outside the receiving area.

Two case studies are considered here in which data describing instantaneous contaminant concentrations in estuarine environments were acquired via field sampling. Both sites feature estuaries dominated by tidal forcing, with smaller, adjacent upland regions also impacted. Metals, particularly copper and lead, are the primary focus in each case. Contaminant transport processes, including diffusion, advection, and bioturbation, are treated together to develop analytical and numerical solutions for time-dependent contaminant concentrations using a spatially varying, time-dependent, effective diffusion coefficient that is influenced by local surface water flow speeds. Different initial, boundary, and loading conditions are considered to illustrate the relative importance of the various transport processes. Implications of future contaminant loading and sea level rise scenarios are demonstrated and discussed.

Keywords Estuaries · Contaminant transport · Metals · Advection, diffusion, bioturbation · Munitions · Sea level rise

P.A. Work (✉) · K.A. Haas
School of Civil and Environmental Eng., Georgia Inst. of Technology, Atlanta, GA, USA
e-mail: pwork@usgs.gov

K.A. Haas
e-mail: khaas@gatech.edu

Present address:
P.A. Work
US Geological Survey, California Water Sci. Ctr., Sacramento, CA, USA

D.A. Warren
Environmental Health Science, University of South Carolina Beaufort, Beaufort, SC, USA
e-mail: dwarren@uscb.edu

Ş. Elci
Department of Civil Engineering, Izmir Institute of Technology, Izmir, Urla, Turkey
e-mail: sebnemelci@iyte.edu.tr

Introduction

The US Environmental Protection Agency (EPA) defines risk assessment as the process of characterizing the "nature and magnitude of health risks to humans and ecological receptors (e.g. birds, fish, wildlife) from chemical contaminants and other stressors that may be present in the environment" (e.g. Wolf 2012). Contaminant solubility is an important characteristic—soluble contaminants are often much more readily transported, and diluted by mixing with surrounding water.

Many contaminants of concern exhibit low solubility in water, but an affinity for sorption to sediment particles. Contaminant transport and transformation is influenced by the fluid mechanics of the overlying water body, sediment transport, sediment and water characteristics, bioturbation, contaminant type, temperature, oxygenation, and other factors.

In most cases it is desired to do one or more of the following:

1. identify regions within an area of interest that have the highest contaminant concentrations
2. define the relative threat posed by one site vs. another
3. identify the vectors by which contaminants migrate off-site, potentially including phase changes, decay, or uptake by organisms
4. identify point(s) of deposition for contaminants migrating off-site

Once the desired steps have been completed to define the scope of the problem, results can be used as a basis to develop a framework for conducting site remediation and/or implementing best management practices for a specific site. Widely used models or model sources include the US EPA Field Environmental Decision Support (FIELDS) analysis and sampling tools, Center for Exposure Assessment Modeling (CEAM) tools (e.g. Bicknell et al. 1993) and the Army Risk Assessment Modeling System (ARAMS; e.g. Johnson et al. 2007). FIELDS combines imaging technologies to describe environmental problems related to human health and ecological risk assessment. CEAM provides predictive exposure assessment techniques for organic chemicals and metals. ARAMS is a modeling system for estimating human and ecological health impacts and risks associated with contaminants.

Site-specific field measurements are often required to determine the existence of exposure pathways between source and receptor of contaminants and for the evaluation of potential remediation options. A few examples are noted here. Kuwabara et al. (2001) conducted a study in Lahontan Reservoir, Nevada that provided direct measurements of the benthic flux of dissolved mercury species (total and methylated forms) between the bottom sediment and water column and specified the potential importance of sediment-water interactions in describing mercury speciation, its sources and sinks. Other work by the same group of researchers involved a pilot study conducted in Lake Coeur d'Alene, Idaho to describe the benthic flux of metals and nutrients into the water column (Kuwabara et al. 1999). They investigated the relative importance of the benthic flux of metals and nutrients in the lake with respect to riverine inputs to decide between the available remedial strategies. Ford et al. (2005) conducted field experiments in the Aberjona Watershed, Massachusetts to investigate the fate of arsenic, lead, and zinc at the groundwater/surface water interface. Their study focused on the assessment of metal speciation transformations in contaminated sediments.

Although the ultimate fate of contaminants will depend on site-specific characteristics and the chemical properties of the contaminants, simplified models can provide guidance for remediation efforts. Liu and Ball (1998) and Zhuang (1997) serve as two examples.

The paper is organized into two broad sections: one that describes the methodology by which two estuarine sites were assessed in the field to quantify contaminant levels at one point in time, and a second that describes an approach for modeling (analytically and numerically) the evolution of contaminant concentration levels within a site, given initial concentrations and other information about the site such as tidal creek geometry and flow speeds. The model makes use of an effective diffusion coefficient that may vary spatially due to bioturbation, the presence of surface water, or other factors. The purpose of this part of the paper is to present and evaluate a modeling strategy that will need to be calibrated for use once a larger dataset is available, i.e. contaminant levels integrated across a site spatially, at multiple points in time.

Field measurements can be used to quantify contaminant concentrations at a given point in time, and two case studies are first presented showing how the authors have done this in estuarine environments. But one-time measurements do not by themselves reveal likely future changes. The complexity of the problem is often such that analytical solutions are generally not realistic because of overly simplified initial or boundary conditions, or forcings. Sophisticated, three-dimensional, time-dependent numerical models exist for quantification of many of the relevant processes, but in some cases a simplified approach is desired for initial assessment, particularly since even the numerical modeling approach can require the collection of a significant amount of data to define initial and boundary conditions, forcing, and calibration parameters.

Both analytical and simplified numerical approaches for treatment of the estuarine contaminant transport problem are considered here. An effective diffusion coefficient is used to account for the combined effects of advection, diffusion, and bioturbation of a conserved contaminant (i.e. bioturbation can enhance transport but does not function as a sink). Different initial conditions are considered, as well as the influence of tidal creeks of varying complexity, and continued contaminant loading.

The developed modeling strategy is applied to an idealized scenario resembling the two estuarine marsh case studies, subject to tidal currents and time-dependent water levels but negligible wave action. Implications of sea level rise are considered; small changes in mean water level are hypothesized to have more significant effects in an intertidal zone than in deeper water or at an upland site.

Case Studies

The authors have been involved in the assessment of several sites, all in coastal regions of the southeastern United States, at which contaminant loading associated with munitions occurred and is in most cases continuing. In each

case the contaminants of interest were low-solubility metals and/or explosives constituents (e.g., perchlorate, RDX) or targets (e.g. clay pigeons). At each site, the primary goal was to quantify the spatial variation in contaminant concentration, which sounds straightforward, but several sites posed significant logistical challenges and required creative sampling techniques. Two sites are considered below, with emphasis on the methodology employed for site assessment rather than specific concentrations or hot spots identified.

Site 1: Tidal Marsh/Creek System Near Rifle/Pistol Range

The first case study is a tidal marsh/creek system that has received extensive small arms fire over the past 100 years and is still heavily used on a nearly daily basis. The primary contaminants of interest were lead and copper, which both exhibit very low solubility in water. Therefore the sampling scheme at this site focused on sediments. The spatial distribution of the contaminant loading was not known a priori but was predicted based on expected projectile trajectories fired from rifle and pistol ranges. The field sampling effort included two primary components: (1) identifying spatial variations in projectile density (i.e. projectiles per unit volume), and (2) quantifying contaminant concentrations and their spatial variations, using the projectile density information to guide the sediment sampling effort. These tasks were completed via two separate field sampling efforts, both of which included resolution of both horizontal and vertical variability in contaminant concentration.

Site 1 is in coastal South Carolina, in a region featuring the largest tidal range in the southeastern United States (mean range 2.4 m). Tidal currents serve as the primary hydrodynamic forcing at the site, and most of the region of interest is in the intertidal zone, although several deeper tidal creeks wind through the site. Sediments in subtidal areas were sampled by vibracoring from a shallow-draft boat, whereas hand coring tools transported on foot were used to sample intertidal areas, at low tidal stages, and upland regions.

Ballistic calculations were used to predict impact zones of the projectiles prior to initial sampling. Rifle range targets were located 6.4 m above the marsh with multiple firing lines at distances of 91, 183, 274, and 457 m from the target. Projectiles of varying caliber have been used throughout the years, although the most common 5.56 mm bullet was assumed for this analysis. Trajectories were calculated using the JBM Small Arms Ballistics model (www.jbmballistics.com; cf. Litz 2009). Different shooter positions were used on the range depending on the distance from the targets: a prone position at 457 m, a kneeling position at 274 m, and a standing position at 91 and 183 m. Corresponding gun barrel heights were assumed to be 15 cm, 50–75 cm, and 1.4–2.0 m above the surveyed ground elevation. To estimate the horizontal extent of the impact zones,

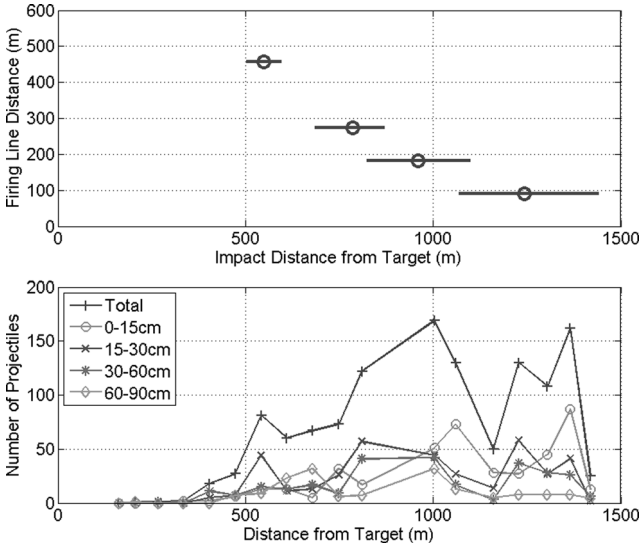

Fig. 1 *Top*: Relationship between firing line distance (shooter distance from target) and predicted distance from target to projectile impact with ground, Site 1. *Circle* corresponds to average height shooter and projectile passing through the center of the target. *Solid line* shows predicted range of distances to impact point. *Bottom*: Excavated projectile counts as a function of distance downrange of the targets, and depth below grade

three different bore angles were assumed to account for: (1) shots made by a small shooter passing 60 cm above the target center line, (2) shots 60 cm below the target center made by a tall shooter, and (3) shots fired through the target center by an average height (1.7 m) shooter.

Sampling sites in the marsh were accessed on foot and a 30 cm diameter by 90 cm deep pit excavated to determine projectile density. Sediments were sampled in four vertical layers: 0–15, 15–30, 30–60, and 60–90 cm below grade to yield the results shown in Fig. 1. Each layer was excavated with a shovel and material placed in a tub. Projectiles were removed by hand for later counting; a metal detector was waved across each handful of pluff mud to ensure that no projectiles had been missed.

Figure 1 shows the predicted impact zones for projectiles, compared to the number excavated manually downrange. Clearly there is a correlation between the predicted bullet impact zones and the observed locations of high projectile densities. Despite the fact that the 91 m firing line was the least frequently used, many projectiles were found within the corresponding impact zone. Based on the trajectories of the bullets fired from the 183 and 274 m positions, many of those bullets should be landing in a creek (∼800 m downrange of the target). At high tide, observations reveal that the high bullet speed and low angle of impact can result in the bullets deflecting off of the water and skipping 200–400 m, landing 1000–1200 m from the target, consistent with Fig. 1.

Fig. 2 PVC corer with check valve ready for unloading, Site 1 intertidal zone

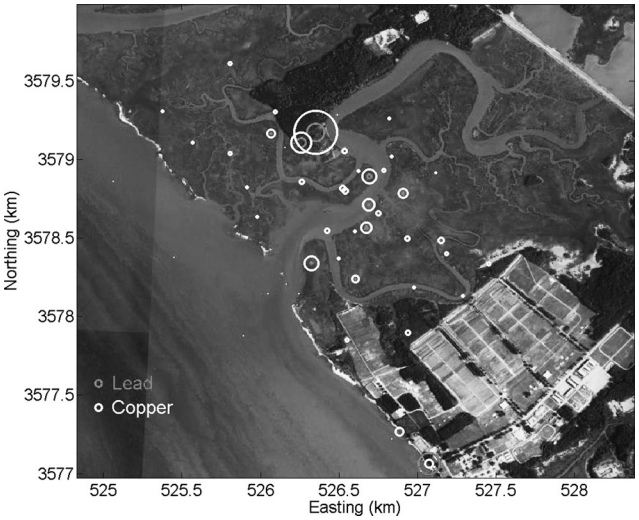

Fig. 3 Lead (*gray circles*) and copper (*white circles*) concentrations in surface sediment samples at Site 1. *Light rectangular areas* at lower right are rifle ranges; *firing direction* is towards the upper left. The *lower left quadrant* is a large tidal river. Size of circles in legend corresponds to toxicological screening values; other circles have diameter proportional to local concentration

Thirty sites were chosen for marsh contaminants analysis. Surface sediments were scooped with a clean, stainless steel spoon directly into a sample container. To extract material from below grade, a 2 m long by 10 cm diameter PVC tube with a manually activated check valve at the bottom was pushed to the depth of interest (Fig. 2). A string was pulled to close the check valve, and the tube pulled out manually. The check valve was unscrewed and the material slid out of the tube into a clean plastic tub for subsampling. A new, clean corer was used for each lift of sediment to eliminate the possibility of cross-contamination between samples.

Twenty-four locations were chosen for vibracoring in subtidal creeks. Steel tubes, 180 cm long by 10 cm diameter, were installed in the vibracorer head, powered by an 11 kW onboard generator. A stainless steel core nose with a core catcher was used to penetrate the creek bed and retain the sample. A flexible plastic liner was used to contain the sample within the tube. The material was sliced into individual lifts in the laboratory and then mechanically mixed for subsampling and analysis.

Subsamples were dried in an oven, pulverized, and analyzed using an X-ray fluorescence (XRF) spectrometer to quantify metals concentrations (US EPA 1998; Method 6200). Per Method 6200, a representative number of samples analyzed via XRF were also sent to a commercial laboratory for analysis by inductively coupled mass spectrometry (ICP-MS) for validation purposes. Additional tests were conducted to define median grain size, soil type, bulk density, organic content, acid volatile sulfide (AVS) and simultaneously extracted metals (SEM). The latter two parameters are considered particularly important as their quantitative relationship serves as a surrogate measure of metals bioavailability (DiToro et al. 1991; US EPA 2005). One common interpretation is that if AVS minus SEM (AVS-SEM) is positive, then the metals are considered fully bound to sediments, with little or no bioavailability to benthic organisms (US EPA 2005). Bioavailability is not considered further here since it is not critical to the modeling discussed below, although it could influence contaminant diffusion coefficients.

The sediment analysis results allowed the production of a map showing metals concentrations versus space for the site, for four different sediment horizons. Figure 3 reveals the spatial variability in the results for copper and lead in the surface horizon. Despite initial expectations based on the ballistics analysis that concentrations would be high within the large creek downrange of the targets, highest concentrations were found at upland areas bordering the marsh at greater distances from the targets. Specific concentrations are not shown but are defined in an extensive report to the sponsor. Subsequent sampling is planned to define time dependence.

Site 2: Estuary Near Skeet Range

The second site was located in the same geographic area as Site 1 and includes similar environmental forcing, but was subjected primarily to small-gauge shot associated with skeet and trap shooting. As at Site 1, upland, intertidal, and subtidal areas were sampled. Lead was the primary contaminant of concern. Augers were used to manually extract upland sediments at Site 2, which contained a larger fraction of sand-sized particles. Intertidal zone sediments were sampled by manual push-coring, and subtidal sediments were collected by vibracoring, resulting in a total of 24 locations

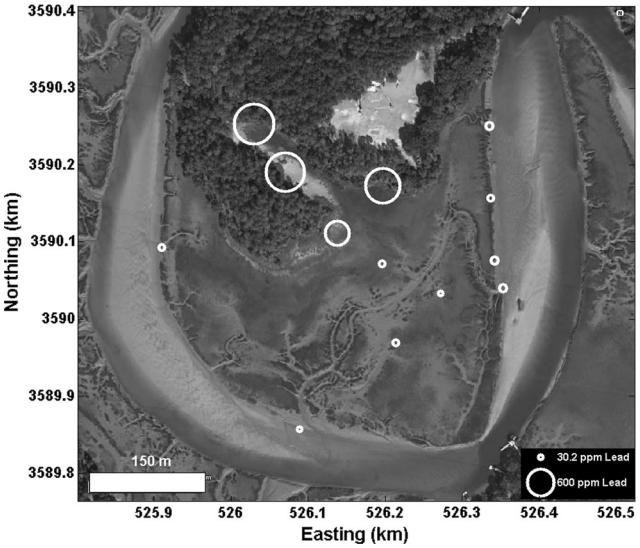

Fig. 4 Lead concentrations exceeding screening value of 30.2 ppm in surface sediment samples at Site 2. Circle diameter is proportional to lead concentration. Firing occurs in bare patch within wooded area at top of figure, directed towards the lower left corner

sampled, with three horizons considered at each site. Background samples were collected at four locations.

Samples were washed through a fine aluminum screen to remove the shot before further analysis. After then filtering to remove the water from the resulting slurry, samples from each of the three horizons (0–15, 15–30, and 30–60 cm) at the 24 horizontal locations were tested for lead, polycyclic aromatic hydrocarbons (PAHs, derived from the clay targets), SEM, AVS, total organic carbon (TOC), and grain size distribution. Figure 4 shows the resulting lead concentrations at sites where they exceeded the toxicological screening value within the surface sediments. Highest concentrations were found in the upland areas that received the largest amount of shot.

Simplified Model

Contaminants within a natural system can be mobilized by a wide variety of mechanisms. If soluble, the contaminant can be advected with porewater or surface water, and diffuse and disperse. If bonded to sediment, it can be transported when the sediment is mobilized. Bioturbation and uptake by biota will also modify concentrations over time, as will chemical reactions.

It is possible to define equations governing each of these processes, and each equation will typically require definition of parameters such as diffusion coefficients based on measurements. Work et al. (2002) considered a scenario featuring simultaneous diffusion, advection, and bioturbation effects on a conserved, soluble contaminant within a simulated creekbed with ostensibly uniform, steady flow. Time-dependent concentrations were simulated with 1- and 2-D diffusion models and an effective diffusion coefficient, lumping together all mixing processes. Advection-dispersion and bioturbation increased the effective diffusivity, as expected.

Many other scenarios have been simplified using diffusion models. Simpson and Schlunegger (2003) considered hillslope erosion, driven by rainfall, which drives sediment into streams, smoothing topography in a diffusive way. Simultaneously, in-stream erosion tends to cut channels and valleys via sediment advection. These competing processes were represented via spatially varying effective diffusion coefficients to simulate watershed evolution.

Here these ideas are effectively combined to yield a model that assumes that contaminant transport in an estuary can be modeled via a spatially varying, effective diffusion coefficient. The spatial variations would arise due to spatial gradients in sediment characteristics, degree of bioturbation, the presence of creeks, and other parameters. One advantage of such an approach is that it is governed by essentially only one scalar parameter, and it is possible in some cases to back-calculate a best-fit value for this parameter from measurements made at different points in time. Note, however, that the numbers that would be used to do this would both contain uncertainty that would influence the computed best-fit effective diffusion coefficient. So a larger dataset would be recommended to reduce uncertainty. At a minimum, it would be necessary to have measurements at two points in time to calibrate the model, and at a third point in time for model validation. The effective diffusion coefficient could be adjusted to minimize the RMS difference between the measured and simulated results.

Consider a marsh system, which for illustrative purposes will be considered circular in planform. It will be assumed subject to temporal changes in water depth, and may feature one or more creeks. Contaminant concentration will be assumed to be initially either spatially uniform or to feature one or more “hot spots” of high concentration. Similarly, the vertical distribution will for now be assumed to be uniform throughout the sediment column, or contained in a single layer at or below the sediment surface. These various scenarios are depicted in Fig. 5. Note that even with contaminants limited to a particular vertical horizon, the problem may in some cases be still essentially 2-D, since some of the relevant processes, such as sediment transport, will primarily lead to horizontal redistribution of contaminants.

Analytical Solution: Quenching Problem

If the contaminant is initially distributed uniformly over the vertical, with zero-flux boundaries at the top and bottom of the sediment column, the problem simplifies to 2-D since no vertical transport occurs. For a conserved contaminant,

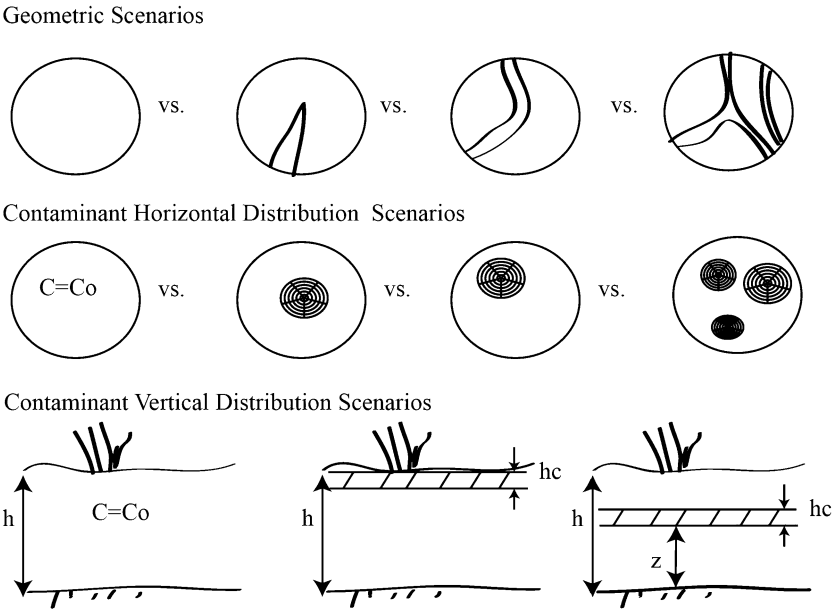

Fig. 5 Simplified scenarios for site geometry and contaminant distributions. *Top row* shows plan view of area with/without tidal creeks; *middle row* shows initial concentrations in planform, and *bottom row* shows profile view of location of contaminated layer of thickness h_c

this problem corresponds to the "quenching problem" considered in heat transfer (e.g. Çengel 2008), with temperature replaced here by contaminant concentration, C, and thermal conductivity by a diffusion coefficient, D, assumed uniform and constant. The equation governing diffusion from the domain can be expressed in polar coordinates as

$$\frac{\partial C}{\partial t} = D\frac{1}{r}\frac{\partial}{\partial r}\left(r\frac{\partial C}{\partial r}\right) \tag{1}$$

where r is radius from the center of the domain. If the initial concentration is uniform and the concentration assumed zero (and constant) on the boundary of the circular domain, and no material added within the domain, an analytical solution for time- and radius-dependent concentration can be expressed in terms of Bessel functions J_o and J_1:

$$C(r,t) = \frac{2C_o}{b}\sum_{n=1}^{\infty}\frac{J_o(\lambda_n r)}{\lambda_n J_1(\lambda_n b)}\exp\left(-D\lambda_n^2 t\right) \tag{2}$$

where b is the radius of the domain, C_o is the initial concentration, and $\lambda_n b$ are the roots of J_o. The fraction of the initial contaminant mass remaining within the domain can be expressed as

$$R(t) = \frac{\int_0^b\int_0^{2\pi} C(r,\theta,t)\,d\theta\,dr}{\int_0^b\int_0^{2\pi} C_o(r,\theta)\,d\theta\,dr} = \frac{4}{b^2}\sum_{n=1}^{\infty}\frac{1}{\lambda_n^2}\exp\left[-D\lambda_n^2 t\right] \tag{3}$$

which for a given geometry depends only on the diffusion coefficient, D, making it possible to determine a best-fit value for diffusion coefficient based on as few as two estimates of R at different times. If an RMS error is defined based on two (or more) pairs of measured vs. predicted values of R, the diffusion coefficient can be adjusted to minimize this RMS error, by trial-and-error or a more sophisticated minimization scheme.

Effective Diffusion in Numerical Solution

Tidally forced flows can lead to contaminant advection, in addition to diffusion. Sediment transport will be assumed proportional to the nth power of flow speed, with a proportionality factor k, and efficiency ϵ. The resulting contaminant flux q_{cx} is assumed proportional to concentration gradient to allow advection to be represented by a spatially varying, effective diffusion coefficient, D_x

$$q_{cx} = D\frac{\partial C}{\partial x} + k\epsilon u_x^n\frac{\partial C}{\partial x} \tag{4}$$

$$D_x = D + k\epsilon u_x^n \tag{5}$$

where u_x is the flow speed in the x-direction. A similar but separate diffusion coefficient D_y is computed for the other horizontal direction, based on flow speed in that direction.

The dimensionless term $\alpha = k\epsilon|u|^n/D$ represents the significance of advection to diffusion in influencing contaminant transport, analogous to a Peclet Number. Bioturbation is not included explicitly but could be introduced by increasing the diffusion coefficient D appearing in Eq. (5), if assumed weakly dependent on flow speed. If more strongly dependent on flow speed, then k in Eq. (5) could be increased instead.

A numerical solution scheme allows inclusion of space- and time-dependence in diffusion coefficient, initial concentration, sources and sinks, and arbitrary boundary conditions. The influence of flow in tidal creeks can also be in-

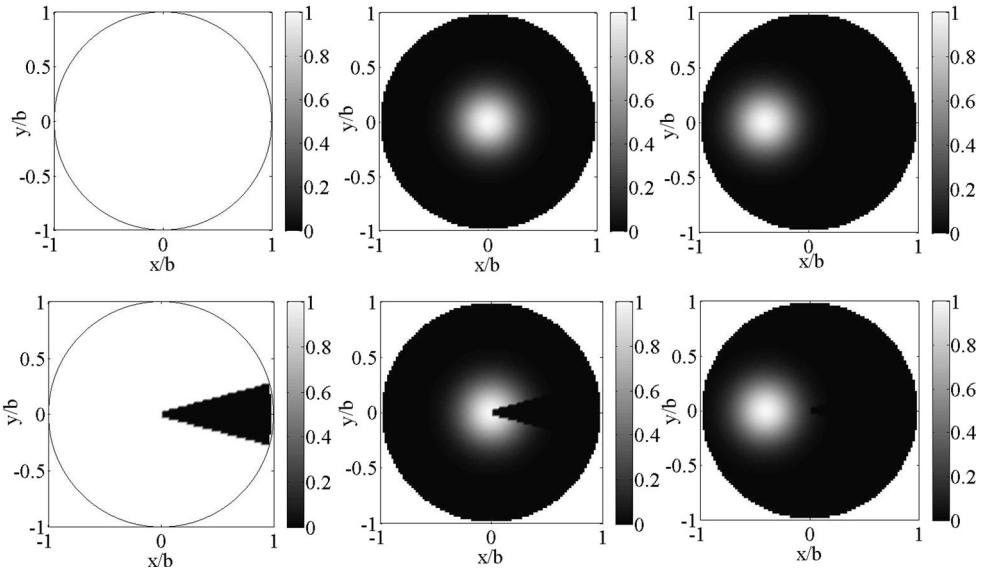

Fig. 6 Initial (dimensionless) concentrations for six cases: uniform, central hot spot, and off-center hot spot (left to right). *Lower row* includes wedge-shaped creek with higher diffusivity and zero initial concentration. *Shade* indicates dimensionless concentration, C/C_o

troduced as shown above. In 2-D Cartesian coordinates the governing equation becomes

$$\frac{\partial C}{\partial t} = \frac{\partial}{\partial x}\left(D_x \frac{\partial C}{\partial x}\right) + \frac{\partial}{\partial y}\left(D_y \frac{\partial C}{\partial y}\right) + g(x, y, t) \tag{6}$$

where a source or sink of strength g has been included. An explicit, first-order, finite-difference scheme was used to solve Eq. (6):

$$\begin{aligned} C_{i,j}^{n+1} = C_{i,j}^{n} &+ \Delta t D_{x_{i,j}} \left[\frac{C_{i+1,j}^{n} - 2C_{i,j}^{n} + C_{i-1,j}^{n}}{\Delta x^2}\right] \\ &+ \Delta t D_{y_{i,j}} \left[\frac{C_{i,j+1}^{n} - 2C_{i,j}^{n} + C_{i,j-1}^{n}}{\Delta y^2}\right] \\ &+ \Delta t \left[\frac{D_{x_{i+1,j}} - D_{x_{i-1,j}}}{2\Delta x}\right]\left[\frac{C_{i+1,j}^{n} - C_{i-1,j}^{n}}{2\Delta x}\right] \\ &+ \Delta t \left[\frac{D_{y_{i,j+1}} - D_{y_{i,j-1}}}{2\Delta y}\right]\left[\frac{C_{i,j+1}^{n} - C_{i,j-1}^{n}}{2\Delta y}\right] \\ &+ \Delta t g_{i,j}^{n} \end{aligned} \tag{7}$$

where i and j denote node numbers in the x- and y-directions, respectively, and n denotes time level. The time step Δt and space steps Δx and Δy are assumed constant but provision has been included for spatial variations in effective diffusion coefficient. This model can be applied for an arbitrary 2-D horizontal domain, with arbitrary initial conditions, variable diffusion coefficients, and contaminant sources and sinks. It could readily be extended to 3-D if the problem warrants, at some expense in computing time.

Figure 6 shows six different initial conditions that were considered. The bottom row includes a wedge-shaped creek; the top does not. In each case, the initial concentration within the creek, where included, is assumed zero. The domains in the left column have uniform initial concentration outside of the creek. The middle column includes a single, central contaminant hot spot as initial condition. The right column features an off-center hot spot. Concentration along the edge of the domain (at all times) is assumed zero in each case. The source/sink term g is also zero for these example cases.

The pseudo-Peclet Number, α, is set to zero everywhere except within the creek, where it is set to 10 for the x-direction. This forces material entering into the creek to be much more quickly carried away by the higher effective diffusion. The fraction of mass remaining within the domain, $R(t)$, is shown in Fig. 7 for each of the six cases defined in Fig. 6. Each simulation was continued until the half-life was reached, i.e. $R(t) = 0.5$. The first two results in Fig. 7 look like the exponential decay predicted by (3). The higher diffusivity of the creek enhances transport out of the domain slightly vs. the no-creek case. When the initial concentration is defined by a hot spot, initial transport out of the domain is slow and then increases at later times as the contaminant reaches the domain boundary. In these cases, the presence of the creek has a more significant effect; it serves as a more efficient escape route for the contaminant.

Surface water flow speeds (dependent on domain geometry, tidal range and tidal prism) and the number and size of the creeks within the system will control the significance of the "advection" term appearing in (4) and the effective diffusion coefficient given by (5). Here only a very simple approach has been used, assuming a single representative flow speed for the entire creek. A separate numerical model could be used to simulate tidal hydrodynamics and results taken as input to the contaminant transport model.

Continuous Loading

The case including a creek and an off-center hot spot as shown in the lower right panel of Fig. 6 was taken as the ini-

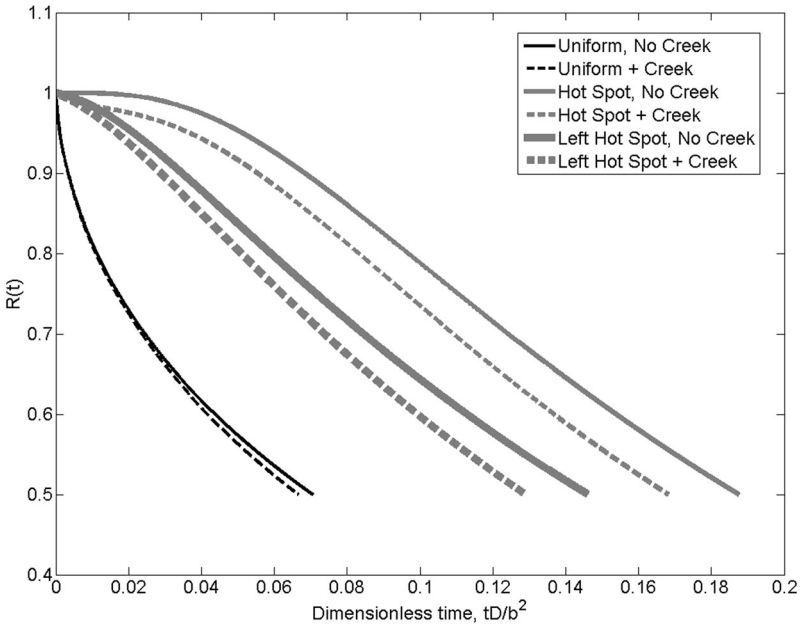

Fig. 7 Fraction mass remaining, R, vs. time for each of the six cases shown in Fig. 6. Time is normalized using ambient diffusion coefficient D and domain radius b, which are the same for each case. Legend defines initial condition and whether tidal creek is included in domain

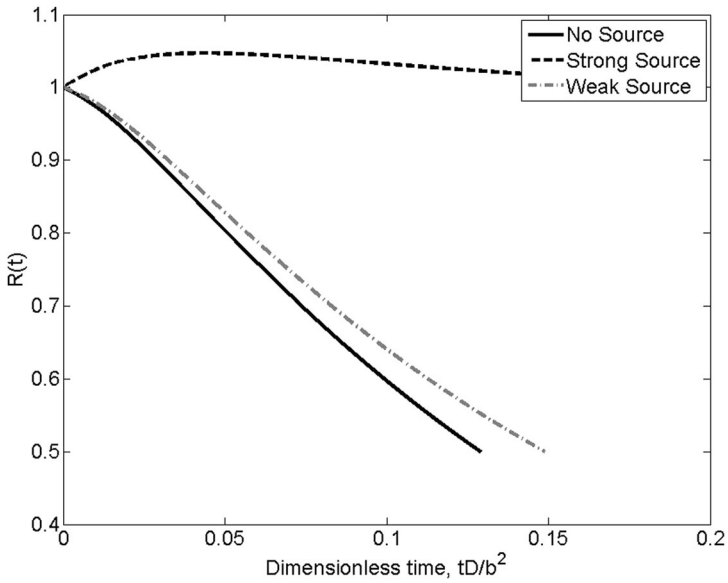

Fig. 8 Fraction mass remaining, R, vs. time for simulations including zero, weak, and strong source terms. Initial condition in each case corresponds to the lower right panel of Fig. 6, with an off-center hot spot and a tidal creek

tial condition for an additional comparison, where the source term appearing in (7) was set to a fixed value at the center of the hot spot. This simulates the effect of continued loading at the site of the initial peak concentration and is thus a bit more like the case studies discussed earlier than the no-source case considered above. Site 1 above has received loading for decades, nearly continuously, although at variable rates. Figure 8 shows the result for cases with strong and weak source terms. A source is considered strong in this example if it leads to an initial increase in mass within the domain (i.e. its magnitude exceeds that of the outward flux along the domain boundary). With a weak source, the nature of the evolution is essentially unchanged; it simply proceeds more slowly. With a strong enough source, the total mass in the domain first increases, followed by a decrease as the concentration moves towards the steady-state solution. Note that for the simplest case with uniform initial concentration and constant diffusion coefficient, the steady-state solution with no source term is $C(r, \theta) = 0$. With a uniform source term (i.e. source added everywhere in the domain, at constant rate), the steady-state solution becomes

$$C(r,\theta) = \frac{1}{4}\frac{gb^2}{D}\left[1 - \left(\frac{r}{b}\right)^2\right] \tag{8}$$

so the concentration varies parabolically with radius. This solution is independent of the initial contaminant level but linearly dependent on the strength of the source, g, and inversely dependent on the diffusion coefficient, D. It corre-

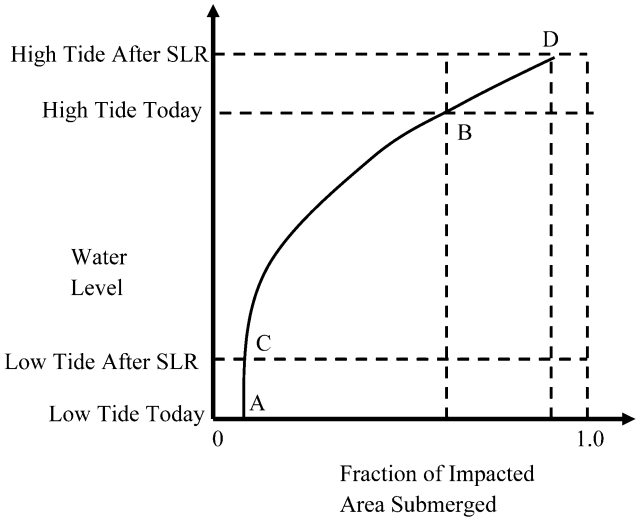

Fig. 9 Hypothetical hypsographic curve for marsh system, and change due to sea level rise (SLR)

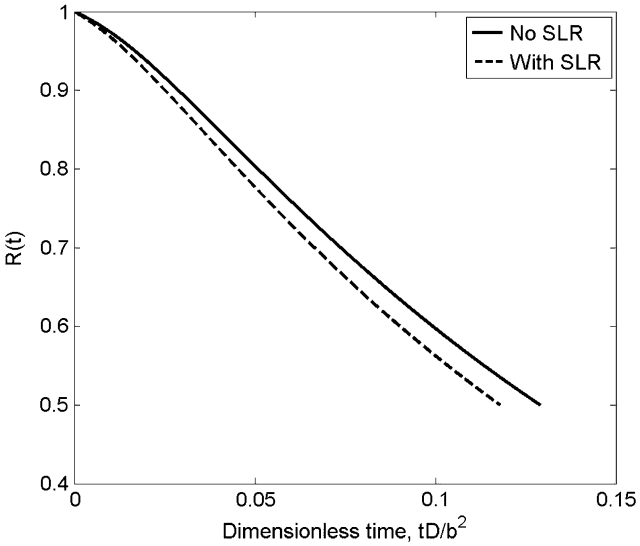

Fig. 10 Influence of sea level rise (SLR) on contaminant transport, assuming that increased depth boosts effective diffusion coefficient in intertidal regions. Initial condition in each case corresponds to the lower right panel in Fig. 6

sponds to the time when the new contaminant loading is exactly balanced by the flux off-site, and would in theory require an infinite amount of time to be reached. Note also that if bioturbation or other processes resulted in a net uptake of contaminant from the domain, this could be represented in the model employed here by inclusion of a contaminant sink as shown in (6).

The two sites considered here as case studies fall between the zero-source case steady-state solution of zero concentration everywhere and the continuous source scenario described by (8). But Site 1, for example, has received loading for decades, with the rate of loading varying somewhat over the years as training requirements have gone up and down. Both sites have received enough loading that loading rates would need to be included for realistic modeling.

Sea Level Rise Influence

A hypsographic curve is often used to show how much area or volume of land or water lies above or below any given elevation of interest. Figure 9 shows a hypothetical hypsographic curve for a marsh system such as those being considered here. At today's low tide level (point A), most of the impact area is subaerial. As the tide rises, the submerged area increases slowly, until the water level exceeds creek bank elevations. Thereafter, submerged area increases rapidly with water level, until a maximum is reached at high tide, marked as point B in the figure.

With sea level rise, the low tide level moves to point C, and high tide to point D, so that a larger fraction of the impacted area would be submerged at high tide. Some areas that were previously above the reach of the tide would now be submerged for a fraction of each tidal cycle, and the lowest parts of what used to be the intertidal zone (above the old low tide level but below the new low tide level, i.e. between points A and C) would be continuously submerged. Contaminant transport that is dependent on sediment transport or bioturbation by aquatic organisms might then be enhanced.

This effect was represented in the model by increasing the effective diffusion in areas lying outside of the tidal creeks, and increasing the flow speed within the creek to account for the larger tidal prism. The effect of the enhanced effective diffusion is shown by comparison to the case without inclusion of sea level rise effects in Fig. 10. The net effect of the sea level rise as modeled here is to increase the effective diffusion coefficient throughout the domain, by an amount similar to when the creek was added to the circular domain. In this case, it was assumed that with sea level rise, creek velocities would be increased ten percent, and flow speeds in the marsh would increase by the same (dimensional) amount as within the creek (from zero). The resulting reduction in contaminant half-life is in this case similar in magnitude to the increase in creek velocities, percentage-wise.

Conclusions

The transport of contaminants into, through, or from estuarine environments is a complicated problem affected by spatially varying and time-dependent physical, chemical, and biological processes. It is possible to represent each of these mathematically, but the resulting model contains a large number of calibration parameters that are often not easily estimated.

Two case studies were considered here. Both correspond to tidal marshes penetrated by tidal creeks, where tidal forcing dominates. One has received small arms fire throughout the past 100 years, sitting downrange of heavily used rifle ranges. The other is downrange of a skeet and trap range and thus also receives metals, but of much smaller caliber. Many potential contaminants were considered, but lead and copper were of primary concern. These contaminants exhibit very low solubility, so tend to move with sediments or as a result of biological activity such as bioturbation.

A diffusion-based, 2-DH (two-dimensional, horizontal) numerical model was developed to simulate contaminant migration from a site, lumping diffusion, advection, and bioturbation effects together into an effective diffusion coefficient. The model was solved using an explicit, finite-difference scheme. Spatial variations in the effective diffusion coefficient were used to simulate the effects of tidal creeks within a marsh system on contaminant transport. Effects of low- and high-level continued contaminant loading were demonstrated.

One simple strategy for consideration of sea level rise effects was introduced. With contaminated regions being submerged for larger fractions of the tidal cycle, the post-sea level rise scenario could result in enhanced effective diffusion coefficients and more rapid contaminant transport out of the domain.

A simplified model such as that developed here can be used to identify future relative concentrations within a site and to help guide field efforts for sampling to identify relative contamination levels. A simple model has the advantage of requiring less data for validation. In theory, a single diffusion coefficient could be computed for the entire domain, if spatial and temporal variations are not large, based on measurements of contaminant mass within the domain for only two points in time. But even determination of these two values is not a trivial task at most sites, as demonstrated with the two case studies considered here. And to reduce uncertainty, the use of a much larger dataset is recommended for model calibration before it is used in a predictive mode. Once this has been done, the model described in this paper allows one to see the relative influence of changes in loading, flow characteristics, or mean water levels on contaminant fluxes.

Acknowledgements This work was funded by the US Marine Corps under contract no. W31RY072216980 to DAW and administered through the Piedmont-South Atlantic Coast Cooperative Ecosystem Studies Unit, of which DoD is a member agency. The authors could like to acknowledge assitance from Hannuman Bull, Kemal Cambazoğlu, Zafer Defne, Thomas Gay, Heidi Hammerstein, Ashley Randall, Adam Sapp, Hampton Simpkins, and Stephanie Smallegan in completing the field work and subsequent sample and data analysis.

References

Bicknell BR, Imhoff JC, Kittle JL, Donigian AS, Johanson RC (1993) Hydrological Simulation Program—FORTRAN (HSPF): users manual for release 10. EPA-600/R-93/174, US EPA, Athens, GA, 30605

Çengel YA (2008) Introduction to thermodynamics and heat transfer, 2nd edn. McGraw-Hill, New York

DiToro DM, Zarba CS, Hansen DJ, Berry WJ, Swartz RC, Cowan CE, Pavlou SP, Allen HE, Thomas NA, Paquin PR (1991) Technical basis for establishing sediment quality criteria for nonionic organic chemicals by using equilibrium partitioning. Environ Toxicol Chem 10(l2):1541–1586

Ford RG, Wilkin RT, Paul CJ, Beck F, Lee T (2005) Field study of the fate of arsenic, lead, and zinc at the ground-water/surface-water Interface. EPA report EPA/600/R-05/161

Johnson MS, Wickwire WT, Quinn MJ, Ziolkowski DJ, Burmistrov D, Menzie CA, Geraghty C, Minnich M, Parsons PJ (2007) Are songbirds at risk from lead at small arms ranges? An application of the spatially explicit exposure model (SEEM). Environ Toxicol Chem 26(10):2215–2225

Kuwabara JS, Berelson WM, Balistrieri LS, Woods PF, Topping BR, Steding DJ, Krabbenhoft DP (1999) Benthic flux of metals and nutrients into the water column of Lake Coeur d'Alene, Idaho. US Geological Survey, Water-resources investigations report 00-4132

Kuwabara JS, Dipasquale MM, Praskins W, Byron E, Topping BR, Carter JL, Fend SV, Parchaso F, Krabbenhoft DP, Gustin MS (2001) Flux of dissolved forms of mercury across the sediment-water interface in Lahontan Reservoir, Nevada. US Geological Survey, Water resources investigations report 02-4138

Litz B (2009) Applied ballistics for long range shooting. Applied Ballistics, LLC

Liu C, Ball WP (1998) Analytical modeling of diffusion-limited contamination and decontamination in a two-layer porous medium. Adv Water Resour 21:297–313

Simpson G, Schlunegger F (2003) Topographic evolution and morphology of surfaces evolving in response to coupled fluvial and hillslope sediment transport. J Geophys Res 108(2300):16. doi: 10.1029/2002JB002162

US EPA (1998) Method 6200: field portable X-ray fluorescence spectrometry for the determination of elemental concentrations in soils and sediments, revision 0, January

US EPA (2005) Procedures for the derivation of Equilibrium Partitioning Sediment Benchmarks (ESBs) for the protection of benthic organisms: metal mixtures (cadmium, copper, lead, nickel, silver and zinc). EPA-600-R-02-011. Office of research and development. Washington, DC

Wolf D (2012) The basics of risk assessment to protect human health and the environment. In: 1st international course-seminar of environmental toxicological pathology, August 23–24

Work PA, Moore P, Reible DD (2002) Bioturbation, advection and diffusion of a conserved contaminant in a laboratory flume. J Water Resour Res Am Geophys Union 38(6):24-1–24-9

Zhuang Y (1997) A semianalytical solution to a diffusion-deposition-resuspension model of local contamination. Atomic Energy of Canada Limited, Chalk River